2-D Encoded Multiplexing Readout for THGEM

Guangyuan Yuan, Shubin Liu, Binxiang Qi, Changqing Feng, and Siyuan Ma

***Abstract*— Micropattern gas detectors (MPGDs) have a wide application in high-energy physics, astrophysics, nuclear physics, medical imaging, and so on. The demand for large area and good spatial resolution requires a large number of channels. The conventional 2-D tracking for MPGDs requires a large number of electronic channels, and in consequence poses a big challenge for the integration, power consumption, cooling, and cost, which has become a problem to the further applications of MPGDs. In this paper, a new tracking method for MPGDs based on 2-D encoded multiplexing readout is presented, which is easily extensible and can significantly reduce the number of electronic readout channels.**

***Index Terms*— 2-D tracking, micropattern gas detector (MPGD), multiplexing readout.**

I. Introduction

MICROPATTERN gas detectors (MPGDs) such as the gas electron multiplier (GEM) [1], the thick GEM (THGEM) [2], and the micromegas [3] are widely used in particle physics. Owing to good spatial resolution, high rate capability, large active area, and radiation hardness, MPGDs also play an important role in high-energy, astrophysics, and medical imaging [4], [5]. To obtain good spatial resolution, the strip size should be reduced and a large effective area requires a large number of channels. The conventional readout techniques [6], usually strips readout, employ a large number of electronic channels. For example, in COMPASS, 5184 readout channels are needed for micromegas and GEM [7]; in ATLAS NSW muon system upgrade, two million readout channels are needed for 1200 m^2 micromegas [8]. The large number of electronic channels results in a big challenge for the integration, power consumption, cooling, and cost.

An encoded multiplexing readout technique was developed by Procureur *et al.* [9] at Saclay, France, which can dramatically reduce the number of electronic readout channels. In our previous work, an easily extensible encoding principle was presented [10]. In this paper, we extend our work to 2-D readout. Verification tests were carried out on a 5×5 cm^2 THGEM [5]. In the verification test, 26 electronic channels are used to read out 100 strips (50 strips in the x-direction and 50 strips in the y-direction), and 30 electronic channels are used to read out 200 strips (100 strips in the x-direction and 100 strips in the y-direction). Up to $2 \times (C_k^2 + 1)$ strips can be read out by $2k$ readout channels (k is odd).

Manuscript received June 24, 2016; revised February 17, 2017, March 27, 2017, and April 5, 2017; accepted May 15, 2017. Date of publication May 23, 2017; date of current version June 26, 2017. This work was supported by the National Natural Science Foundation of China under Grant 11222552. *(Corresponding author: Guangyuan Yuan.)*

The authors are with the State Key Laboratory of Particle Detection and Electronics, University of Science and Technology of China, Hefei 230026, China (e-mail: liushb@ustc.edu.cn).

Color versions of one or more of the figures in this paper are available online at http://ieeexplore.ieee.org.

Digital Object Identifier 10.1109/TNS.2017.2706766

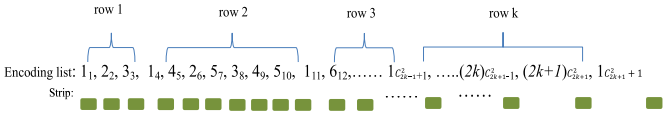

Fig. 1. Encoding list of channels and strips. The form x_y represents each multiplexing connection, where x is the electronic channel number and y is the strip number along the detector.

II. Principle and Method

A. Encoding Principle

In our previous work, an easily extensible 1-D encoded multiplexing readout for MPGDs is presented [10]. By using the redundancy that each particle usually showers the signal on several neighboring strips in MPGDs, a feasible and easily extensible way of encoding and decoding has been developed for MPGD, and a general formula of encoding and decoding for n channels is derived.

The encoding list is shown in Table I. A row shows when readout channels are added from $2k+1$ to $2k+3$, up to $4k+3$ more strips can be encoded. Fig. 1 shows the encoding list for $2k+1$ readout channels, corresponding with $C_n^2 + 1$ strips. This method of encoded multiplexing readout can be easily extended to large number of readout channels

$$(a,b) = \begin{cases} \left(\dfrac{R+1}{2}, 2k\right) & R = 4m+1,\ m = 0, 1 \ldots k-1 \\ \left(2k, \dfrac{R+2}{2}\right) & R = 4m+2,\ m = 0, 1 \ldots k-1 \\ \left(\dfrac{R+1}{2}, 2k+1\right) & R = 4m+3,\ m = 0, 1 \ldots k-1 \\ \left(2k+1, \dfrac{R+2}{2}\right) & R = 4m+4,\ m = 0, 1 \ldots k-1 \\ (2k+1, 1) & i = C_{2k+1}^2 \end{cases} \tag{1}$$

$$(i)_{ab} = \begin{cases} c_b^2 & b \text{ is odd},\ a = 1 \\ c_{b-2}^2 + 2a - 2 & b \text{ is odd},\ a \neq 1 \text{ and } a \text{ is odd} \\ c_{b-2}^2 + 2a - 1 & b \text{ is odd},\ a \text{ is even, and } b - a \neq 1 \\ c_{b-2}^2 + 2a - 2 & b \text{ is odd},\ b - a = 1 \\ c_{b-1}^2 + 2a - 1 & b \text{ is even},\ a \text{ is odd} \\ c_{b-1}^2 + 2a - 2 & b \text{ is even},\ a \text{ is even}. \end{cases} \tag{2}$$

TABLE I
ENCODING LIST OF MULTIPLEXING CONNECTIONS

row	list of encoded multiplexing connections
1	1_1, 2_2, 3_3
2	1_4, 4_5, 2_6, 5_7, 3_8, 4_9, 5_{10}
3	1_{11}, 6_{12}, 2_{13}, 7_{14}, 3_{15}, 6_{16}, 4_{17}, 7_{18}, 5_{19}, 6_{20},7_{21}
.	.....
k	$1C^2_{2k-1+1}$, $(2k)C^2_{2k-1+2}$, $2C^2_{2k-1+3}$, $(2k+1)C^2_{2k-1+4}$, $3C^2_{2k-1+5}$, $(2k)C^2_{2k-1+6}$.....$(2k\text{-}1)C^2_{2k+1\text{-}2}$, $(2k)C^2_{2k+1\text{-}1}$, $(2k+1)C^2_{2k+1}$ $1C^2_{2k+1}+1$

The encoded connections list by row. Add a new row on the list when two new channels are added.

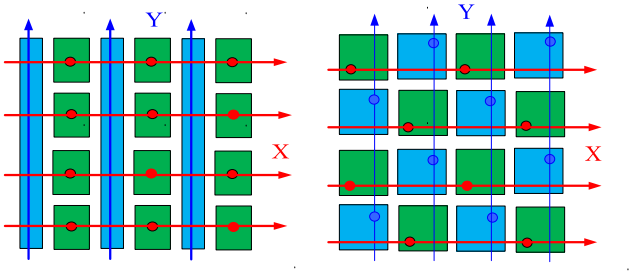

Fig. 2. 2-D readout construction. Readout anode structure as pads and strips is shown in the left, while structure as pads is shown in the right.

Formula (1) shows the encoding rule. Readout channels (a, b) are connected with neighbor hit strips i and $i+1$. $R = i - C^2_{2k-1} = i - (k-1)(2k-1)$.k is the minimal positive integer meeting formula $k+1 \geq (1+\sqrt{1+4i}/2)$.

Formula (2) shows the decoding rules when two channels are fired. While channel a and channel b are fired, strip i and $i+1$ can be uniquely decoded.

The situation when more than two channels are fired is also discussed in our previous work. As shown in Table I and Fig. 1, when three channels are fired, such as channel 2, 3, and 5, the position can be uniquely decoded to strip 6, 7, 8. Details are described in [10].

B. 2-D Tracking

In a 2-D tracking situation, this encoding method can be easily extended. We make a further step in our research and a 2-D readout is presented. Using 2-D orthogonal strips readout as charge collection electrode, encoding horizontal strips, and vertical strips respectively, reading out the signals and decoding to get the hit strips, then synthesizing the results we implement 2-D readout. Fig. 2 shows two different electrode constructions for 2-D readout anode.

In order to verify our method, two types of encoded multiplexing anode readout printed circuit board (PCB) are manufactured with different anode structure and a different number of readout strips. Several anode strips are connected to one electronic readout channel by encoding principle on the PCB.

1) Anode Structure as Pads: Anode structure as pads is applied in the design of 50 × 50 readout PCB, as shown in Fig. 3. In each direction, 13 electronic channels are used to read out 50 strips, and 26 electronic channels are used to read out all 2500 pads. The connections of strips and readout channels are shown in Table II.

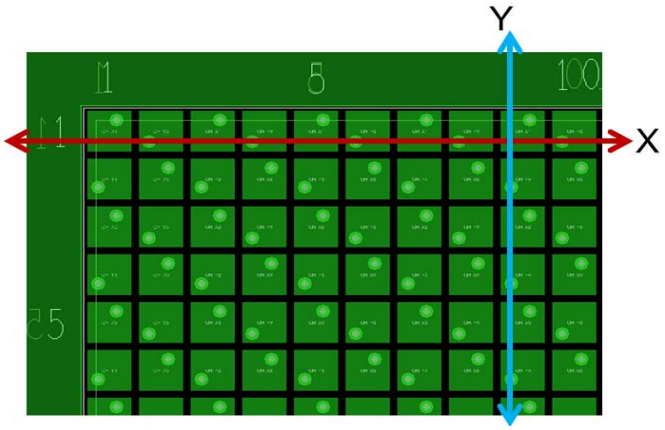

Fig. 3. Readout electrode as pads. A 5 × 5 cm^2 active area is divided into 50 × 50 pads (1 × 1 mm^2 each).

TABLE II
ENCODING LIST OF 50 READOUT STRIPS

row	the list of encoded multiplexing connections
4	1_1,8_2,2_3,9_4,3_5,8_6,4_7,9_8,5_9,8_{10},6_{11},9_{12},7_{13},8_{14},9_{15}
5	1_{16}, 10_{17}, 2_{18}, 11_{19}, 3_{20}, 10_{21}, 4_{22}, 11_{23}, 5_{24}, 10_{25}, 6_{26}, 11_{27}, 7_{28}, 10_{29}, 8_{30}, 11_{31}, 9_{32}, 10_{33}, 11_{34}
6	1_{35}, 12_{36}, 2_{37}, 13_{38}, 3_{39}, 12_{40}, 4_{41}, 13_{42} ,5_{43},12_{44}, 6_{45}, 13_{46}, 7_{47}, 12_{48}, 8_{49}, 13_{50}

TABLE III
ENCODING LIST OF 100 READOUT STRIPS

row	list of encoded multiplexing connections
2	1_1,4_2,2_3,5_4,3_5,4_6,5_7
3	1_8,6_9,2_{10},7_{11},3_{12},6_{13},4_{14},7_{15},5_{16},6_{17},7_{18}
4	1_{19},8_{20},2_{21},9_{22},3_{23},8_{24},4_{25},9_{26},5_{27},8_{28},6_{29},9_{30},7_{31},8_{32},9_{33}
5	1_{34}, 10_{35}, 2_{36}, 11_{37}, 3_{38}, 10_{39}, 4_{40}, 11_{41}, 5_{42}, 10_{43}, 6_{44}, 11_{45}, 7_{46}, 10_{47}, 8_{48}, 11_{49}, 9_{50}, 10_{51}, 11_{52}
6	1_{53}, 12_{54}, 2_{55}, 13_{56}, 3_{57}, 12_{58}, 4_{59},.....,7_{65}, 12_{66}, 8_{67}, 13_{68},9_{69},12_{70}, 10_{71}, 13_{72}, 11_{73}, 12_{74}, 13_{75}
7	1_{76}, 14_{77}, 2_{78}, 15_{79}, 3_{80}, 14_{81} ,4_{82},15_{83}.....,10_{94},15_{95}, 11_{96}, 14_{97}, 12_{98}, 15_{99}, 13_{100}

2) Anode Structure as Pads and Strips: To improve spatial resolution, we apply a new structure of readout anode in the design of 100 × 100 readout PCB, as shown in Fig. 4. Fifteen electronic channels are used to read out 100 strips in each direction. Ten thousand equivalent pads are read out by 30 electronic channels. The encoded multiplexing connection list is shown in Table III.

III. VERIFICATION TEST

A. Test Platform

In order to verify this method, X-ray imaging verification tests were carried out on a 5 cm × 5 cm THGEM detector using Ar/iC_4H_{10} (97:3) gas mixture. It has a hole

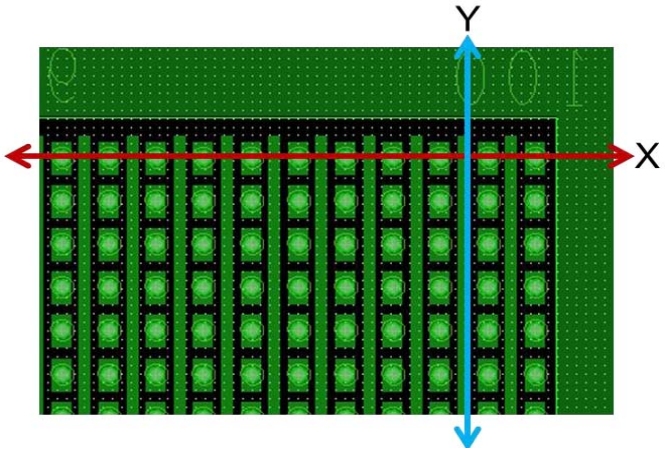

Fig. 4. Readout electrode as pads and strips. In a 5 × 5 cm^2 active area, anodes in the y-direction are designed in strips while strips in the x-direction are designed in pads, with equivalent pad area of 0.5 × 0.5 mm^2.

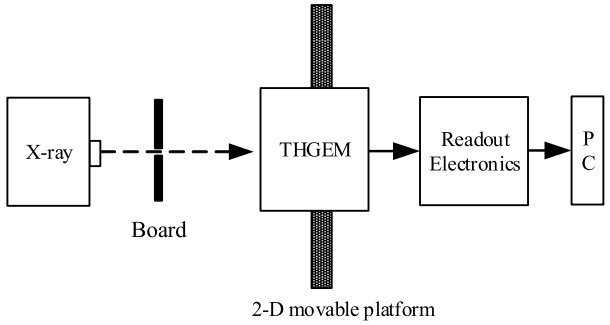

Fig. 5. Test platform structure. An 8-keV Cu X-ray beam passes through Cu board engraved with letters to the detector. Then read out signals are selected by encoded anode PCB.

diameter of $d = 200$ μm, spaced by $a = 500$ μm. The thickness is $t = 200$ μm. The detector was biased to a total gain of 1×10^4. The output signal of THGEM detector is about 5–100 fC, with system noise better than 2 fC. A 100-μm-wide slit in a thin brass sheet was used to produce a miniaturized X-ray beam. A manual movable platform was used for the position scanning test. The test platform structure is shown in Fig. 5. Two different types of readout anode PCB are designed to collect the signals of detector, one with 1-mm-wide pitch and another one with 0.5-mm-wide pitch. Finally by decoding the channels' signals we get the hit position and rebuild the pictures, thus 2-D imaging is implemented.

B. Test Result

We apply electronics based on the VATA160 chip to read out the signals, which can offer charge quantity on each channel [11]. When decoding to get the hit position, we apply a charge gravity method to improve spatial resolution. Q_i is the quantity of electric charge on readout strip I, and b_i is the baseline of electronics

$$I_G = \frac{\sum (Q_i - b_i) I_i}{\sum (Q_i - b_i)}. \tag{3}$$

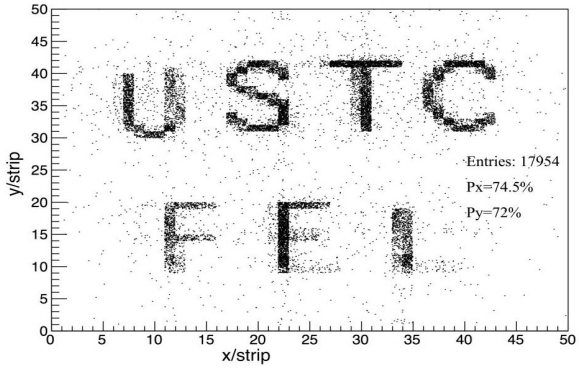

Fig. 6. Imaging result of 50 × 50 readout anode PCB.

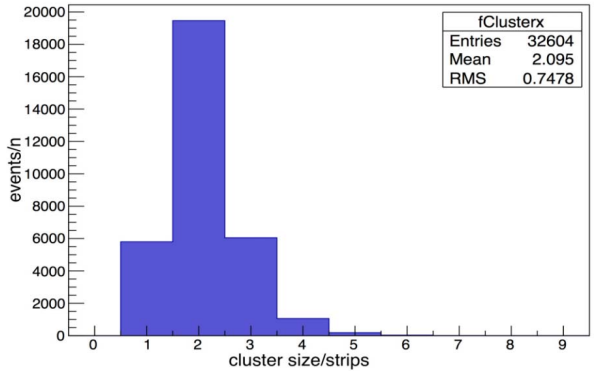

Fig. 7. Cluster size distribution in the x-direction, result of 50 × 50 readout electrode as pads, 1 × 1 mm^2 each, equivalent 1-mm pitch.

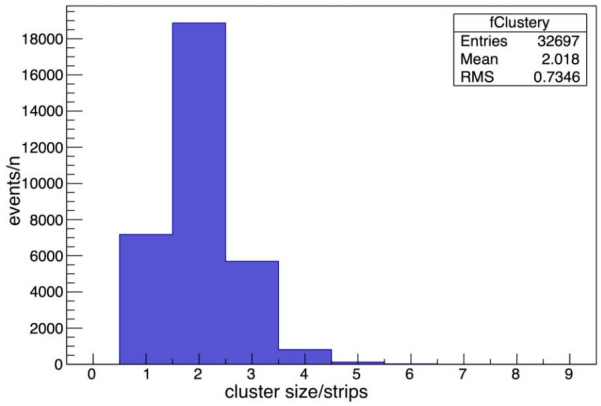

Fig. 8. Cluster size distribution in the x-direction, result of 50 × 50 readout electrode as pads, 1 × 1 mm^2 each, equivalent 1-mm pitch.

In this method, the number of fired channels is important in decoding to get the hit position. Besides, the spatial resolution and imaging result is used to measure the feasibility of this method.

1) 50 × 50 Readout Result: Fig. 6 is the rebuilt image of 50 × 50 anode readout PCB. The threshold of electronics is set to 20 fC, three times that of the baseline noise (7 fC). In the x-direction, about 19% of events hit have only one channel fired and cannot be decoded. In the y-direction the rate is about 20%. When two channels records signals, such as channels 3 and 5, we can uniquely decode the position to strips 4, 5 by Table III; when three channels records signals,

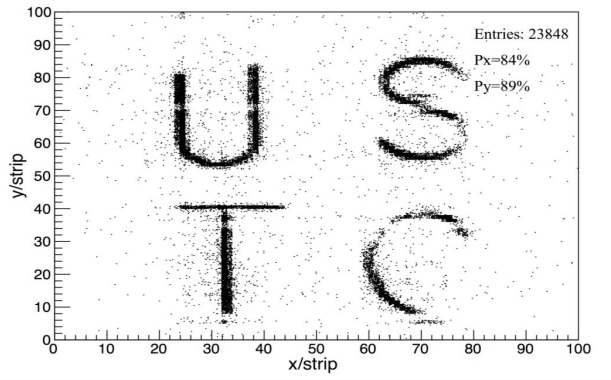

Fig. 9. Imaging result of 100 × 100 readout anode PCB.

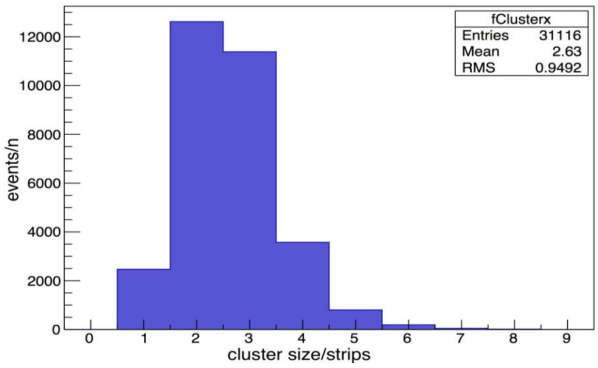

Fig. 10. Cluster size distribution in the x-direction, result of 100 × 100 readout electrode as pads, equivalent 0.5-mm pitch.

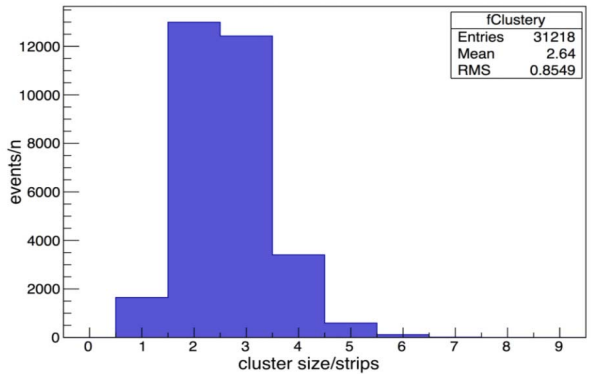

Fig. 11. Cluster size distribution in the y-direction, result of 100 × 100 readout electrode as strips in the y-direction, 0.5-mm pitch.

such as 3, 4, and 6, we can uniquely decode the position to strips 12, 13, 14. On the other side, when four strips are fired, such as 1, 2, 3, and 4, then channels 1, 2, 4, 5 will record signals, we can uniquely decode the position to strip 1, 2, 3, 4.

Position rms in the x-direction is 0.7478 strip (0.7478 mm), and that in the y-direction is 0.7346 strip (0.7346 mm). Figs. 7 and 8 show the cluster size distribution in x- and y-directions.

2) 100 × 100 Readout Result: Fig. 9 is the rebuilt image of 100 × 100 anode readout PCB. The threshold of electronics is set to 20 fC, three times that of the baseline noise. In the x-direction, about 7% of events hit only have one channel fired and cannot be decoded. In the y-direction the rate is about 6%. The results are shown in Figs. 10 and 11.

Position rms in the x-direction is 0.95 strip (0.475 mm), and in the y-direction is 0.85 strip (0.425 mm). The result shows that encoded multiplexing readout method is feasible for 2-D tracking. Lower-noise electronics are indispensable if we want a clearer image.

IV. Conclusion

The test results show this method has a good performance in 2-D imaging for THGEM and can be easily extended to a large number of readout strips. But there are still some places to be improved. As can be seen from the result of the two tests, smaller readout pads will help to get better spatial resolution and reduce the rate that some events cannot be decoded. Besides, the image rebuilt is not clear enough. We need electronics with lower noise to get clearer image.

As this 2-D readout method can dramatically reduce the number of readout channels, it has an attractive potential to help build MPGDs with a large number of readout strips. Moreover, it can also have a wide range of position imaging applications such as medical imaging and industry.

References

[1] F. Sauli, "GEM: A new concept for electron amplification in gas detectors," *Nucl. Instrum. Methods Phys. Res. A, Accel. Spectrom. Detect. Assoc. Equip.*, vol. 386, pp. 531–534, Feb. 1997.

[2] A. Breskin *et al.*, "A concise review on THGEM detectors," *Nucl. Instrum. Methods Phys. Res. A, Accel. Spectrom. Detect. Assoc. Equip.*, vol. 598, pp. 107–111, Jan. 2009.

[3] Y. Giomataris *et al.*, "MICROMEGAS: A high-granularity position-sensitive gaseous detector for high particle-flux environments," *Nucl. Instrum. Methods Phys. Res. A, Accel. Spectrom. Detect. Assoc. Equip.*, vol. 376, pp. 29–35, Jun. 1996.

[4] M. Titov, "New developments and future perspectives of gaseous detectors," *Nucl. Instrum. Methods Phys. Res. A, Accel. Spectrom. Detect. Assoc. Equip.*, vol. 581, pp. 25–37, Oct. 2007.

[5] Q. Liu *et al.*, "A successful application of thinner-THGEMs," *J. Instrum.*, vol. 8, no. 11, Nov. 2013. [Online]. Available: http://iopscience.iop.org/article/10.1088/17480221/8/11/C11008/meta

[6] A. Bressan *et al.*, "Two-dimensional readout of GEM detectors," *Nucl. Instrum. Methods Phys. Res. A, Accel. Spectrom. Detect. Assoc. Equip.*, vol. 425, pp. 254–261, Apr. 1999.

[7] P. Abbon *et al.*, "The COMPASS experiment at CERN," *Nucl. Instrum. Methods Phys. Res. A, Accel. Spectrom. Detect. Assoc. Equip.*, vol. 577, pp. 455–518, Jul. 2007.

[8] G. Iakovidis, "The micromegas project for the ATLAS upgrade," *J. Instrum.*, vol 8, no. 12, Dec. 2013. [Online]. Available: http://iopscience.iop.org/article/10.1088/17480221/8/12/C12007/meta

[9] S. Procureur, R. Dupré, and S. Aune, "Genetic multiplexing and first results with a 50×50 cm^2 Micromegas," *Nucl. Instrum. Methods Phys. Res. A, Accel. Spectrom. Detect. Assoc. Equip.*, vol. 729, pp. 888–894, Nov. 2013.

[10] B.-X. Qi *et al.*, "A novel method of encoded multiplexing readout for micro-pattern gas detectors," *Chin. Phys. C*, vol. 40, no. 5, pp. 58–62, May 2016.

[11] C. Feng *et al.*, "Design of the readout electronics for the BGO calorimeter of DAMPE mission," *IEEE Trans. Nucl. Sci.*, vol. 62, no. 6, pp. 3117–3125, Dec. 2015.